


**Information scrambling in quantum walks: Discrete-time formulation of Krylov complexity**Himanshu Sahu <sup>\*</sup>*Department of Physics and Department of Instrumentation & Applied Physics, Indian Institute of Science, Bangalore-560012, Karnataka, India;**Perimeter Institute for Theoretical Physics, Waterloo, Ontario, Canada N2L 2Y5;**and Department of Physics and Astronomy and Institute for Quantum Computing, University of Waterloo, Ontario, Canada N2L 3G1*

(Received 11 June 2024; revised 4 October 2024; accepted 17 October 2024; published 4 November 2024)

We study information scrambling (a spread of initially localized quantum information into the system's many degree of freedom) in discrete-time quantum walks. We consider out-of-time-ordered correlators (OTOC) and K complexity as a probe of information scrambling. The OTOC for local spin operators in all directions has a light-cone structure which is "shell-like." As the wavefront passes, the OTOC approaches to zero in the long-time limit, showing no signature of scrambling. The introduction of spatial or temporal disorder changes the shape of the light-cone akin to localization of wavefunction. We formulate the K complexity in system with discrete-time evolution, and show that it grows linearly in discrete-time quantum walk. The presence of disorder modifies this growth to sublinear. Our study present interesting case to explore many-body phenomenon in a discrete-time quantum walk using scrambling.

DOI: [10.1103/PhysRevA.110.052405](https://doi.org/10.1103/PhysRevA.110.052405)**I. INTRODUCTION**

Quantum scrambling [1,2] is the process where interactions within a quantum system spread local information across its many degrees of freedom. It's a fundamental process behind how isolated quantum systems reach thermal equilibrium [3–5], and it's closely linked to quantum chaos [6], the black-hole information problem [7–9], and how disorder affects collective spins in many-body systems [10,11]. The concept of scrambling also lays the groundwork for developing algorithms in quantum benchmarking and machine learning, which can make the exploration of Hilbert spaces more efficient [12–16].

There remain ambiguity is describing the process of quantum scrambling. One method to probe it involves using an out-of-time-ordered correlator [1,17]. For systems that exhibit a semi-classical limit or have a large number of local degrees of freedom, this correlator shows exponential growth, which can be used to identify a quantum counterpart to the Lyapunov exponent (LE), thus linking it to classical chaos [18]. Another approach involves studying the evolution dynamics of operators in Krylov space. Here, operator growth is measured by the "K-complexity," indicating the extent of delocalization of initial local operators evolving under Heisenberg evolution under the system Hamiltonian [19–21]. It is speculated that this K-complexity grows exponentially in most generic nonintegrable systems [19]. This exponential growth in K-complexity can be used to extract LE, establishing a connection with out-of-time-ordered correlators [6]. Recent studies have explored K-complexity in various systems such as Ising models [22–24], Sachdev-Ye-Kitaev

(SYK) models [25–27], quantum field theories [28–33], the many-body localization system [34,35], and open quantum systems [36–40].

Experimentally tunable toy models serve as valuable tools for investigating different phenomena from theoretical physics. One such tool, which we will pursue in this work, is the quantum walk (a quantum version of the classical random walk [41,42]). Specifically, we examine discrete-time quantum walks, which were previously employed to simulate controlled dynamics in quantum systems [43–45] and to construct quantum algorithms [42]. These quantum walks are implemented experimentally using both lattice-based quantum systems and circuit-based quantum processors [46–48]. The adaptability of quantum walks, allowing for the experimental modeling of various phenomena like topological effects [45,49], therefore, also positions them as a promising platform for studying scrambling.

In this article, we study the out-of-time-ordered correlator (OTOC) and K-complexity for different operators in the exactly solvable one-dimensional discrete-time quantum walk. Our study of OTOC for different spin operators shows a universal "shell-like" structure so as the wavefront passes, the OTOC goes to zero in the long-time limit, in other words, the operator has no support on the site, implying the absence of scrambling (see Fig. 1). However, we show that K-complexity grows linearly in time, akin to the approximate orthonormality of operator at each time step. We further study the effect of disorder which generally results in the slowdown of information scrambling. In both spatial and temporal disorder, the shape of the light-cone deforms, showing no scrambling beyond localization length. The K-complexity growth transitions from linear to sublinear, showing saturation at late times, thus reflecting the localization of the operator.

<sup>\*</sup>Contact author: [hsahu@perimeterinstitute.ca](mailto:hsahu@perimeterinstitute.ca)

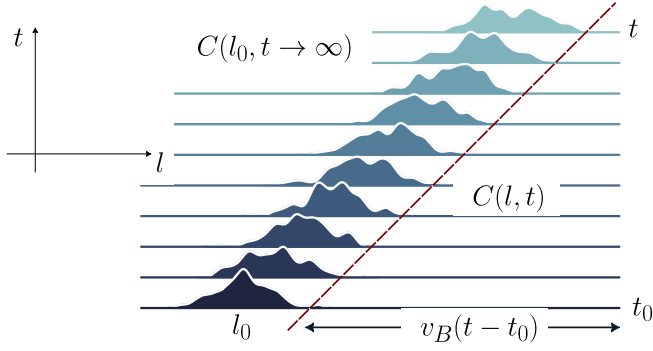


FIG. 1. Schematic showing the “shell-like” structure of OTOC in which, as the wavefront passes the operator site  $l$ , the OTOC approaches to zero in the long-time limit. The horizontal line shows different time slices increasing in an upward direction. We note that the site where OTOC is nonzero at initial time, goes to zero at late time, implying that the operator has no support on site.

## II. QUANTIFYING SCRAMBLING

### A. Out-of-time-ordered correlators

OTOCs provide a means to quantify the evolution of operators. Let's consider two local operators,  $W$  and  $V$ , within a one-dimensional spin chain. The idea is to probe the spread of  $W(t) = e^{iHt} W e^{-iHt}$  using another operator  $V$ , typically a simple spin operator positioned at a distance  $l$  from  $W$  evolving under system Hamiltonian  $H$ . To do this, we consider the expectation value of the squared commutator

$$C(l, t) = \langle [W(t), V]^\dagger [W(t), V] \rangle. \quad (1)$$

Initially, this quantity is zero for widely separated operators, but it deviates significantly from zero once  $W(t)$  extends to the location of  $V$ . In the special scenario where  $W$  and  $V$  are Hermitian and unitary, the squared commutator can be expressed as  $C(t) = 2 - 2 \text{Re} [\langle W(t) V W(t) V \rangle]$ , with  $\langle W(t) V W(t) V \rangle = F(t)$  representing the OTOC. The growing interest in OTOCs has spurred numerous experimental proposals and experiments aimed at measuring them [50–55].

The OTOC serves as a tool to investigate characteristics of chaos such as operator growth and the butterfly effect. In the case of local interactions, the growth  $C(l, t)$  is conjectured to obey [10,56–58]

$$C(l, t) \sim \exp \left[ -\lambda_p \frac{(l - v_B t)^{1+p}}{t^p} + a \log t \right]. \quad (2)$$

Here,  $v_B$  denotes the butterfly velocity,  $p$  represents the wavefront broadening coefficient, and  $a$  encapsulates the logarithmic growth observed in the many-body localized (MBL) phase under disorder.

### B. Krylov complexity

#### 1. Continuous-time evolution

In a closed system, the evolution of any operator  $\mathcal{O}_0$  under a time-independent Hamiltonian  $H$  is described by the

Heisenberg equation of motion

$$\mathcal{O}(t) = e^{iHt} \mathcal{O}_0 e^{-iHt} = e^{i\mathcal{L}t} \mathcal{O}_0 = \sum_{n=0}^{\infty} \frac{(it)^n}{n!} \mathcal{L}^n \mathcal{O}_0, \quad (3)$$

where  $\mathcal{L}$  is the Hermitian Liouvillian superoperator given by  $\mathcal{L} = [H, \bullet]$ . Therefore, the operator  $\mathcal{O}(t)$  can be written as a span of the nested commutators with the initial operator, i.e.,  $\{\mathcal{L}^n \mathcal{O}_0\}_{n=0}^{\infty}$ . An orthonormal basis  $\{|O_n\rangle\}_{n=0}^{K-1}$  can be constructed from this nested span of commutators by choosing a certain scalar product  $(\cdot | \cdot)$  on operator space using a form of Gram-Schmidt orthogonalization known as the Lanczos algorithm. The dimension of Krylov space  $K$  obeys a bound  $K \leq D^2 - D + 1$ , where  $D$  is the dimension of the state Hilbert space [21]. In the Krylov basis  $\{|O_n\rangle\}$ , the Liouvillian takes the tridiagonal form  $\mathcal{L}|O_n\rangle = b_{n+1}|O_{n+1}\rangle + b_n|O_n\rangle$ , where  $b_n$  are known as the Lanczos coefficients that are tied to chaotic nature of the system at hand [23]. We can write the expansion of the operator  $\mathcal{O}(t)$  in terms of the constructed Krylov basis as

$$\mathcal{O}(t) = \sum_{n=0}^{K-1} i^n \phi_n(t) |O_n\rangle. \quad (4)$$

The amplitudes  $\phi_n(t)$  evolve according to the recursion relation  $\phi_n(t) = b_{n-1} \phi_{n-1}(t) - b_n \phi_{n+1}(t)$  with the initial conditions  $\phi_n(0) = \delta_{n,0}$ . The recursion relation suggests that the Lanczos coefficients  $b_n$  are hopping amplitudes for the initial operator  $\mathcal{O}_0$  localized at the initial site to explore the *Krylov chain*. With time, the operator gains support away from the origin in the Krylov chain reflects the growth of complexity as higher Krylov basis vectors are required in operator expansion. To quantify this, one defines the average position of the operator in the Krylov chain, called the Krylov complexity, as

$$K(t) = [\mathcal{O}(t) | \mathcal{K} | \mathcal{O}(t)] = \sum_{n=0}^{K-1} n |\phi_n(t)|^2, \quad (5)$$

where  $\mathcal{K} = \sum_{n=0}^{K-1} n |O_n\rangle \langle O_n|$  is the position operator in the Krylov chain. For our purpose, we will use the infinite-temperature inner product, also known as/the Frobenius inner product

$$(\mathcal{A} | \mathcal{B}) = \frac{1}{D} \text{Tr}[\mathcal{A}^\dagger \mathcal{B}], \quad \|\mathcal{A}\| = \sqrt{(\mathcal{A} | \mathcal{A})}. \quad (6)$$

#### 2. Discrete-time evolution

To formulate the K-complexity for a system with discrete-time evolution such that  $\mathcal{O}_n = U_n^\dagger \mathcal{O}_{n-1} U_n = \mathcal{U}_n[\mathcal{O}_n]$ , where  $n = 1, 2, \dots$ ,  $U_n$  is the unitary operator which describes the evolution of the system at time step  $t = nT$  with step size  $T$ , and  $\mathcal{U}_n$  is the unitary superoperator given by  $\mathcal{U}_n = U_n^\dagger \bullet U_n$ . We define the Krylov basis by choosing  $|O_0\rangle = \mathcal{O}_0$  and then recursively orthogonalizing each  $\mathcal{O}_n$  with all the  $|O_n\rangle$  for  $i < n$ . This choice of basis (represented by  $\mathbb{O}$ ) maximizes the cost function defined as [59]

$$K_{\mathbb{B}}(t) = \sum_i \zeta_i |(\mathcal{O}_t | \mathbb{B}_i)|^2, \quad (7)$$

with respect to an arbitrary choice of orthonormal set  $\mathbb{B} = \{|\mathbb{B}_i\rangle : i = 0, 1, 2, \dots\}$ . The coefficients  $\zeta_i$  (referred to as the

“weight function”) are positive, increasing the sequence of real numbers. The optimal choice of the basis follows from the induction method. We fix the initial state as the first state of the Krylov basis  $\mathcal{O}_0 = |O_0\rangle$ . Assume the first  $N$  vectors of certain basis  $\mathbb{B}$  are the same as the Krylov basis, i.e.,  $|B_i\rangle = |O_i\rangle$  for  $i = 0, 1, \dots, N - 1$ . By assumption

$$\mathcal{O}_n = \sum_{j=0}^{N-1} (K_j | \mathcal{O}_n) | O_j \rangle \quad n \leq N - 1.$$

Therefore, the cost associated with the two bases are the same for  $n \leq N - 1$ . The next state  $|O_N\rangle$  into a part belonging to the Krylov subspace  $|O_i\rangle$ , for  $i \leq N - 1$ , and a part perpendicular to it, i.e.,

$$\mathcal{O}_N = p_{\perp} |O_N\rangle + p_{\parallel} |O_{\parallel}\rangle, \quad |O_{\parallel}\rangle = \sum_{i=0}^{N-1} a_i |O_i\rangle,$$

where  $|O_N\rangle$  is the next element of the Krylov basis by definition. A basis different from the Krylov one would necessarily not include  $|O_N\rangle$ . Therefore, the cost at discrete time  $N$  would be larger since we would have to express  $|K_N\rangle$  in the new basis, which would require at least two vectors. Since the contribution to the cost from the part  $|O_{\parallel}\rangle$  is the same in both bases, the cost must increase when we divide  $|O_N\rangle$  into several contributions since  $\zeta_n$  is a strictly increasing function of  $n$ . Therefore, the Krylov basis minimizes the cost function for all times.

At any time  $t = nT$ , we can expand the state  $\mathcal{O}_t$  in the Krylov basis as

$$\mathcal{O}_n = \sum_{i=0}^{D^2} \phi_{i,n} |O_i\rangle, \quad (8)$$

where the expansion coefficient  $\phi_{i,t} = (O_i | \mathcal{O}_n)$ . We define the K-complexity of the state as the average position of the distribution on the ordered Krylov basis

$$K(t) = \sum_{i=0}^{D^2} i |\phi_{i,n}|^2. \quad (9)$$

Since the evolution operator itself is used as a generator of the Krylov basis, we can bound the maximum possible growth of the K-complexity. *For any system evolving unitarily in discrete time, the K-complexity can grow, at most, linearly with time  $t$ .* To prove this, we consider maximizing the complexity at anytime  $t$  with respect to the expansion coefficients, i.e.,

$$\max_{\{\phi_{i,n}\}} K(t) = \max_{\{\phi_{i,n}\}} \sum_i i |\phi_{i,n}|^2, \quad (10)$$

with constraint  $\sum_i |\phi_{i,n}|^2 = 1$ . From the orthonormalization construction, it follows that the expansion coefficients  $\phi_{i,n} = 0 \forall i > n$ . Therefore, it follows that the complexity can, at most, grow linearly with time  $t$  corresponding to the case where  $\phi_{i,n} = \delta_{i,n}$ . In terms of the operator, it means that  $(O_{n'} | O_n) \forall n' < n$ , which corresponds to the maximally ergodic regime universal in chaotic systems [60].

In the case where the evolution operator is time independent, we can define a quasi-Hamiltonian  $H_q$  such that  $U = e^{-iH_q T}$ . In this case, the unitary operator  $U$  takes the

upper Hessenberg form in the Krylov basis [60], given by

$$(O_i | U | O_j) = \begin{cases} 0 & \text{if } j > i + 1, \\ b_j & \text{if } j = i + 1, \\ a_j c_i / c_j & \text{if } j < i + 1, \end{cases} \quad (11)$$

with  $a_0 = c_0$ . The quasi-Hamiltonian  $H_q$  can itself be used in the continuous-time setting to define complexity using the notion discussed in Sec. II B 1. To investigate the relation between the complexities, we consider the following expansion:

$$e^{i\mathcal{L}_q T} = \sum_{k=0}^{\infty} \frac{(iT)^k}{k!} \mathcal{L}_q^k \approx \sum_{k=0}^{K_c} \frac{(iT)^k}{k!} \mathcal{L}_q^k, \quad (12)$$

where  $\mathcal{L}_q$  is the Liouvillian superoperator associated with the Hamiltonian  $H_q$ . The Taylor series is truncated at order  $K_c$ , which depends on the operator  $\mathcal{L}_q$ , step size  $T$ , and error tolerance [61]. From Eq. (12), it follows that the operator at first time step  $\mathcal{O}_1$  will be a linear combination of operators  $\{\mathcal{L}_q^k \mathcal{O}_0 \mid k = 0, 1, \dots, K_c\}$ . In other words, the first Krylov basis vector

$$|O_1\rangle = \sum_{k=0}^{K_c} \psi_{k,1} |O_k^{(q)}\rangle, \quad (13)$$

where the set  $\mathbb{O}^{(q)} = \{|O_k^{(q)}\rangle \mid k = 0, 1, \dots\}$  corresponds to the Krylov basis associated with the Liouvillian  $\mathcal{L}_q$ . In general, we will assume that there exists a cutoff value  $K_c^{(i)}$  such that

$$|O_i\rangle = \sum_{k=0}^{K_c^{(i)}} \psi_{k,i} |O_k^{(q)}\rangle, \quad (14)$$

$$\mathcal{O}_n = \sum_{i=0}^n \phi_{i,n} |O_i\rangle = \sum_{k=0}^{K_c^{(n)}} \phi_{k,n}^{(q)} |O_k^{(q)}\rangle. \quad (15)$$

Therefore, the K-complexity associated with the Liouvillian  $\mathcal{L}_q$  (refer to as the *quasi-K-complexity*) given by

$$\begin{aligned} K^{(q)}(t) &= \sum_{k=0}^{K_c^{(n)}} k |\phi_{k,n}^{(q)}|^2 = \sum_{k=0}^{K_c^{(n)}} k \left| \sum_{i=0}^n \phi_{i,n} \psi_{k,i} \right|^2 \\ &\leq \sum_{k=0}^{K_c^{(n)}} k \sum_{i=0}^n |\phi_{i,n}|^2 |\psi_{k,i}|^2 \\ &= \sum_{i=0}^n \left( \sum_{k=0}^{K_c^{(n)}} k |\psi_{k,i}|^2 \right) |\phi_{i,n}|^2. \end{aligned} \quad (16)$$

Therefore, the quasi-K-complexity  $K^{(q)}(t)$  is similar to that of the unitary operator with a modified weight factor  $\zeta_i$ . The suitable choice of weight factor to recover the quasi-K-complexity is nontrivial and depends on the growth of wave functions  $\phi_{k,n}^{(q)}$ . Let us consider the case where the wave function grows exponentially  $|\phi_{k,t}^{(q)}|^2 \sim e^{-k/\xi(t)}$ , where  $\xi(t)$  is the delocalization length that grows exponentially in time  $\xi(t) \sim e^{2\alpha t}$  for  $\alpha t \gg 1$ , corresponding to the exponential growth (maximum possible growth) of the quasi-K-complexity [19]  $K^{(q)}(t) \sim e^{2\alpha t}$ . To retain this growth, one possible choice of

weight function is  $\zeta_i = e^{2\alpha i}$  along with the maximal growth of wave function  $\phi_{i,n} = \delta_{i,n}$ .

We will now consider the limiting case where step size  $T \rightarrow 0$  to recover the continuous limit. In this case,  $e^{i\mathcal{L}_q T} \approx I + iT\mathcal{L}_q$ , up to the correction of order  $\mathcal{O}(T^2)$ , therefore, the Krylov basis generated by unitary operator  $U$  and quasi-Liouvillian  $\mathcal{L}_q$  matches exactly to each other. However, it should be noted that the two complexities will eventually start to differ at large time step as the errors start to accumulate and grow large.

### III. DISCRETE-TIME QUANTUM WALKS

The discrete-time quantum walk on a line is defined on a Hilbert space  $\mathcal{H} = \mathcal{H}_c \otimes \mathcal{H}_p$  where  $\mathcal{H}_c$  is the coin Hilbert space and  $\mathcal{H}_p$  is the position Hilbert space. For a walk in one dimension,  $\mathcal{H}_c$  is spanned by the basis set  $|\uparrow\rangle$  and  $|\downarrow\rangle$  representing the internal degree of the walker and  $\mathcal{H}_p$  is spanned by the basis state of the position  $|x\rangle$  where  $x \in \mathbb{Z}$  on which the walker evolves. At any time  $t$ , the state can be represented by

$$|\Psi(t)\rangle = |\uparrow\rangle \otimes |\Psi^\uparrow(t)\rangle + |\downarrow\rangle \otimes |\Psi^\downarrow(t)\rangle = \sum_x \begin{bmatrix} \psi_{x,t}^\uparrow \\ \psi_{x,t}^\downarrow \end{bmatrix}. \quad (17)$$

Each step of the discrete-time quantum walk is defined by a unitary quantum coin operation  $C$  on the internal degrees of freedom of the walker followed by a conditional position shift operation  $S$  which acts on the configuration of the walker and position space. Therefore, the state at time  $(t+1)$  will be

$$|\Psi(t+1)\rangle = S(C \otimes I)|\Psi(t)\rangle = W|\Psi(t)\rangle. \quad (18)$$

The general form of coin operator  $C$ , given by

$$C = C(\xi, \theta, \varphi, \delta) = e^{i\xi} e^{-i\theta\sigma_x} e^{-i\varphi\sigma_y} e^{-i\delta\sigma_z}, \quad (19)$$

where  $\xi$  is the global phase angle;  $2\theta, 2\varphi, 2\delta$  are the angles of rotation along the  $x, y$ , and  $z$  axes, respectively, with  $\theta, \varphi, \delta \in [0, 2\pi]$ ; and  $\sigma^\mu$  is the  $\mu$ th component of the Pauli spin matrices  $\{\sigma_x, \sigma_y, \sigma_z\}$ , which are generators of the  $SU(2)$  group. The position shift operator  $S$  is of the form

$$S = |\downarrow\rangle\langle\downarrow| \otimes T_+ + |\uparrow\rangle\langle\uparrow| \otimes T_-, \quad T_\pm = \sum_{x \in \mathbb{Z}} |x \pm 1\rangle\langle x|, \quad (20)$$

which are translation operators. In this work, we will consider the specific choice of coin operator

$$C(\theta) = \begin{bmatrix} \cos \theta & \sin \theta \\ -\sin \theta & \cos \theta \end{bmatrix}, \quad (21)$$

corresponding to parameters  $(0, \theta, 0, 3\pi/2)$  which previously was studied in the context of the Dirac dynamic [62]. In momentum basis, the unitary operator can be diagonalized to obtain the dispersion relation in the space-time continuum limit [63]

$$\omega(k, \theta) = \pm \sqrt{k^2 \cos \theta + 2(1 - \cos \theta)}. \quad (22)$$

Therefore, the group velocity  $v_g(k, \theta)$  given by

$$v_g(k, \theta) \equiv \frac{d\omega(k, \theta)}{dk} = \pm \frac{k \cos \theta}{\sqrt{k^2 \cos \theta + 2(1 - \cos \theta)}}. \quad (23)$$

It's important to note that the group velocity is maximum (equals 1) at  $\theta = 0$  for all  $k$  which corresponds to the identity as coin operator. The coin parameter  $\theta$  controls the variance  $\sigma^2$  of the probability distribution in the position space, and this distribution spreads quadratically faster ( $\sigma^2 \approx [1 - t^2 \sin \theta]$ ) in position space when compared to the classical random walk [64].

#### Disordered discrete-time quantum walk

There are a number of ways to induce disorder in the discrete-time quantum walk that usually lead to localization of the wave function [65–70]. Here, we will consider two choices of disorder: spatial and temporal disorder. The spatial disorder in the quantum walk is defined by introducing a position-dependent coin operator  $C(\theta_x)$  with  $\theta_x \in \theta_0 + \{-W/2, W/2\}$  where  $0 \leq W \leq \pi$  defines the disorder strength and  $\theta_0$  is the mean value. Therefore, the evolution of the state is described by

$$|\Psi(t+1)\rangle = S \bigoplus_x C(\theta_x) |\Psi(t)\rangle. \quad (24)$$

In a similar analogy, the temporal disorder in the quantum walk is defined by introducing a time-dependent coin operator  $C(\theta_t)$  with  $\theta_t \in \theta_0 + \{-W/2, W/2\}$ . The evolution of the state is given by

$$|\Psi(t+1)\rangle = S[C(\theta_t) \otimes I] |\Psi(t)\rangle. \quad (25)$$

While the temporal disorder in a quantum walk leads to a weak localization, the spatial disorder is known to induce Anderson localization [67]. Although, in both cases,

$$\lim_{t \rightarrow \infty} \langle v_g^{\text{SD/TD}} \rangle \rightarrow 0. \quad (26)$$

The mean group velocity drops to zero faster for a walk with spatial disorder, resulting in strong localization compared to temporal disorder which leads to weak localization. The localization length is usually a function of the coin parameter  $\theta$  given as  $\zeta = [\ln \cos \theta]^{-1}$ . Both of these disorders were studied extensively in enhancing the entanglement and non-Markovianity generated between the internal and external degrees of freedom [70,71].

## IV. RESULTS

### A. Out-of-time-ordered correlator

We will be interested in the quantities

$$C_{\mu\nu}(l, t) \equiv \frac{1}{2} \langle |[W_l^\mu(t), V_0^\nu]|^2 \rangle \\ = \frac{1}{2} \langle [W_l^\mu(t), V_0^\nu]^\dagger [W_l^\mu(t), V_0^\nu] \rangle, \quad (27)$$

where  $\mu, \nu \in \{x, y, z\}$ , and the operators  $W_l^\mu$  and  $V_0^\nu$  are local operators defined as  $\sigma^\mu \otimes |l\rangle\langle l|$  and  $\sigma^\nu \otimes |0\rangle\langle 0|$ , respectively.

We consider the function  $C_{\mu\nu}(l, t)$  in Eq. (27) for the discrete-time quantum walk in one dimension and coin angle  $\theta$  for varying distance  $l$  between the initial operators. Figure 2 shows the numerical results for  $C_{\mu\nu}(l, t)$  at various time slices. We can identify the velocity of the wavefront as  $v_B = \max_k d\epsilon_k/dk = \max_k v_g(k, \theta)$ . It follows that the light cone grows linearly with maximum velocity  $v_B = 1$  corresponding to  $\theta = 0$ . In continuous systems, the

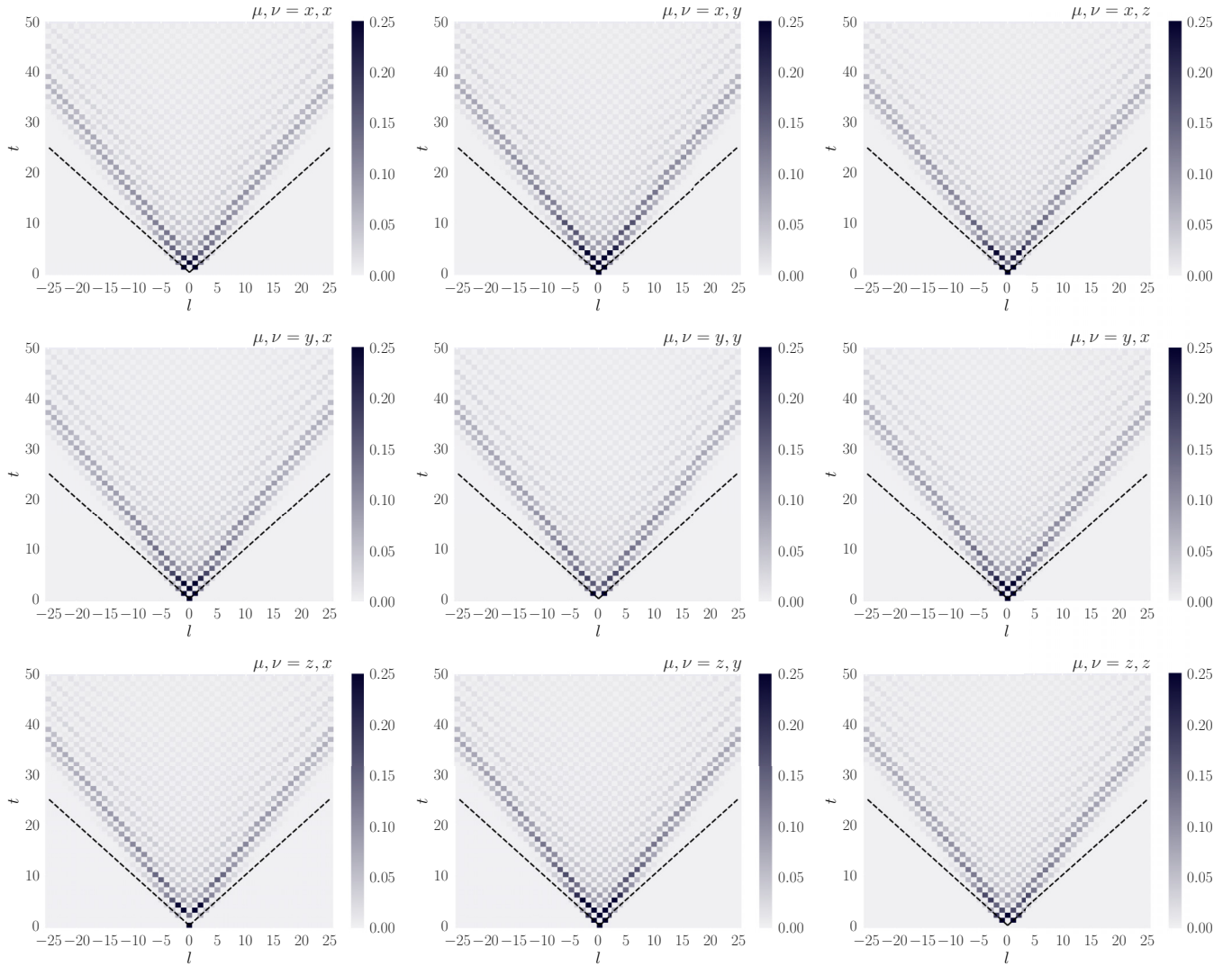


FIG. 2. The function  $C_{\mu\nu}(l, t)$  for the discrete-time quantum walk; the system size is  $L = 100$ ; the coin-angle  $\theta = \pi/4$ . We show data as the matrix plot as a function of  $l$  and time  $t$  (the maximum is set to 0.25 in all cases for better visibility and comparison). The light cone can be readily identified and corresponds to the maximal quasiparticle group velocity  $v_B = \max_k d\epsilon_k/dk$ . In the time-like region,  $C_{\mu\nu}(l, t)$  approaches zero in the long-time limit, indicating the absence of “scrambling.” The dotted lines show the light cone corresponding to case  $v_B = 1$  corresponding to the case  $\theta = 0$ .

long-range interaction can result in superlinear growth of the light cone [1]. Therefore, in principle, the long-range connectivity in discrete-time evolution can also result in superlinear growth of the light cone. In the present case, the OTOC function is “shell-like.” That is, inside the time-like region, in the long-time limit,  $C_{\mu\nu}(l, t) \rightarrow 0$ , indicating no scrambling of operator  $W_l^\mu(t)$ , the vanishing of the  $C_{\mu\nu}$  OTOC in the long-time limit suggests that the expansion of  $W_l^\mu(t)$  in terms of Pauli strings does not contain many Pauli matrices “in the middle” of the strings. The feature common to integrable quantum systems [72]. Additionally, in the case of a quantum walk, we find that the function  $C_{\mu\nu}$  oscillates between a finite value and zero, which stems from the form of the shift operator and the choice of initial operators.

In integrable systems such as quantum spin systems [72], one can analytically find the squared commutator to exactly describe the nature of the wavefront and decay. In addition, although, quantum walk is also an integrable model, it turns

out to be particularly hard to find out the exact form of squared commutator. This is because the initial operators are local in position space, and the inverse Fourier transform becomes hard due to the complexity of functions. However, in the case of the Hadamard quantum walk ( $\theta = \pi/4$ ), we can use the known asymptotic results of the wave function to vaguely argue the nature of decay and the wavefront [73]. To this end, the asymptotics for the wave function can be described in three regions using  $\alpha = l/t$ . The wave function is essentially uniformly spread over the interval between  $\mp 1/\sqrt{2} = \mp v_B$  where its gross behavior is like  $1/\sqrt{t}$ . Outside this interval, the wave function dies out much faster than any inverse polynomial in  $t$ . At the “wavefront” ( $\pm v_B$ ), there are two peaks of width  $\mathcal{O}(t^{1/3})$ , where the wave function goes as  $t^{-1/3}$ . If we approximately translate these wave-function behaviors to operator  $W_l^\mu(t)$ , we conclude that the squared commutator decays as  $\sim 1/t^2$  in the long-time limit and goes to as  $t^{-4/3}$  at the wavefront.

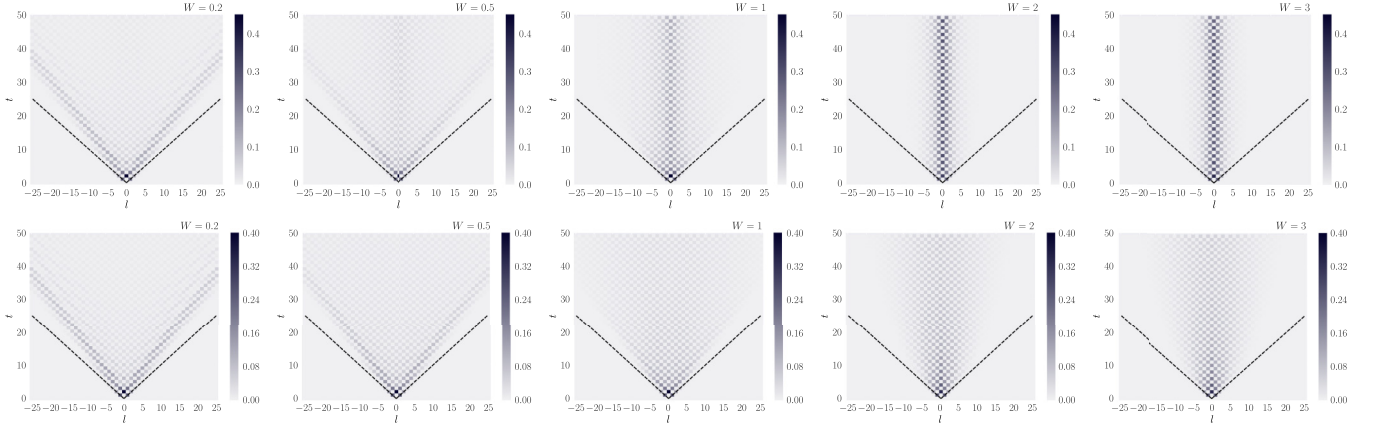


FIG. 3. The function  $C_{xt}(l, t)$  for the discrete-time quantum walk in presence of spatial (top) and temporal (bottom) disorder; the system size is  $L = 100$ ; the disorder strength  $W$ . The disorder average is taken over 500 realizations.

The disorder (both spatial and temporal) in a system causes a slowdown in information propagation (see Fig. 3). In particular, the spatial disorder results in Anderson localization should be distinguished from the MBL phase. The latter is known as a noninteracting phenomenon. As the disorder strength increases, the shape of the light cone changes from ballistic to confined up to localization length for time  $t \rightarrow \infty$ , showing no information propagation beyond localization length. As shown in Fig. 3, the spatial disorder leads to more rapid localization compared to temporal disorder as we increase disorder strength.

To characterize the localization, we consider the inverse participation ratio (IPR) defined as [74]

$$\text{IPR}(t) = \sum_x |\langle x | \Psi(t) \rangle|^4 = \sum_x p_x^2(t), \quad (28)$$

where  $p_x(t)$  is the probability of the walker being at position  $x$  and time  $t$ . The IPR quantifies the number of basis states that effectively contribute to the system's time evolution. Figure 4 shows the IPR calculated in the presence of spatial and temporal disorder for varying disorder strength  $W$ . In the presence of disorder, the IPR saturates to a finite value which increases with disorder strength. The saturation value is larger in the case of spatial compared to temporal disorder, showing that localization is strong in the presence of spatial disorder.

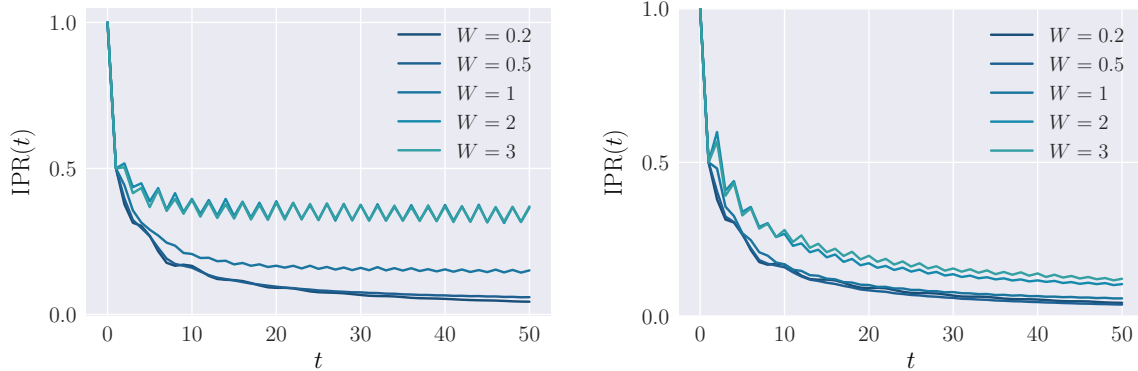


FIG. 4. Inverse participation ratio calculated for spatial (left) and temporal (right) disorder with varying disorder strength  $W$ . The disorder average is taken over 500 realizations.

## B. K-complexity

Considering the formulation of the K-complexity presented in Sec. II B for discrete-time evolution, we can show that the discrete-time quantum walk exhibit linear growth. We will consider the initial operator to be of the form  $\mathcal{O}_0 = \sigma^\mu \otimes |0\rangle\langle 0|$ . At any time  $t$ , the operator is given by (we will fix the step size  $T$  to unity)

$$\mathcal{O}_t = (U^\dagger)^t \mathcal{O}_0 U^t, \quad (29)$$

where the evolution operator  $U = S(C \otimes I)$ . We will show that the set of operators  $\{\mathcal{O}_0, \mathcal{O}_1, \mathcal{O}_2, \dots\}$  form an orthogonal basis i.e.,  $(\mathcal{O}_i | \mathcal{O}_j) = \delta_{ij}$ . First, we note that operators  $\{P_{ij} \equiv |i\rangle\langle j| : i, j \in \mathbb{Z}\}$  form an orthogonal basis in position Hilbert space  $\mathcal{H}_p$ . Next, consider the operator  $\mathcal{O}_1 = U^\dagger \mathcal{O}_0 U$ ,

$$\begin{aligned} \mathcal{O}_1 &= (C^\dagger \otimes I \cdot S^\dagger) \mathcal{O}_0 (S \cdot C \otimes I) \\ &= C_\downarrow^\dagger \sigma^\mu C_\downarrow \otimes |-1\rangle\langle -1| + C_\downarrow^\dagger \sigma^\mu C_\uparrow \otimes |-1\rangle\langle 1| \\ &\quad + C_\uparrow^\dagger \sigma^\mu C_\downarrow \otimes |1\rangle\langle -1| + C_\uparrow^\dagger \sigma^\mu C_\uparrow \otimes |1\rangle\langle 1|, \end{aligned}$$

where  $C_\uparrow = |\uparrow\rangle\langle \uparrow| C$  and  $C_\downarrow = |\downarrow\rangle\langle \downarrow| C$  to unclutter the notation and we use  $T_\pm^\dagger = T_\pm$ . More generally, the evolution of operator  $|l\rangle\langle l|$  contains the linear combination of terms  $|l \pm 1\rangle\langle l \pm 1|$  that are orthonormal to each other. In what

follows, it will prove important to represent the operators as

$$\mathcal{O}_0 = \begin{array}{cccccc} \bullet & \bullet & \bullet & \bullet & \bullet & \bullet \\ \bullet & \bullet & \bullet & \bullet & \bullet & \bullet \\ \bullet & \bullet & \bullet & \bullet & \bullet & \bullet \\ \bullet & \bullet & \bullet & \bullet & \bullet & \bullet \\ \bullet & \bullet & \bullet & \bullet & \bullet & \bullet \\ \bullet & \bullet & \bullet & \bullet & \bullet & \bullet \end{array} \quad \mathcal{O}_1 = \begin{array}{cccccc} \bullet & \bullet & \bullet & \bullet & \bullet & \bullet \\ \bullet & \bullet & \bullet & \bullet & \bullet & \bullet \\ \bullet & \bullet & \bullet & \bullet & \bullet & \bullet \\ \bullet & \bullet & \bullet & \bullet & \bullet & \bullet \\ \bullet & \bullet & \bullet & \bullet & \bullet & \bullet \\ \bullet & \bullet & \bullet & \bullet & \bullet & \bullet \end{array}, \quad (30)$$

where the blue dot represents the presence of the term  $P_{ij} = |i\rangle\langle j|$  and the multiple presence of blue dot represents the linear combination of these terms in operator expansion. The inner product between operators  $\mathcal{O}_i$  and  $\mathcal{O}_j$  depends on the expansion term corresponding to where the dot color matches. The inner product between the operators in Eq. (30) is zero, i.e., the operators are orthonormal to each other since there are no common blue dots. At  $t = 2, 3$ , the operators are given by

$$\mathcal{O}_2 = \begin{array}{cccccc} \bullet & \bullet & \bullet & \bullet & \bullet & \bullet \\ \bullet & \bullet & \bullet & \bullet & \bullet & \bullet \\ \bullet & \bullet & \bullet & \bullet & \bullet & \bullet \\ \bullet & \bullet & \bullet & \bullet & \bullet & \bullet \\ \bullet & \bullet & \bullet & \bullet & \bullet & \bullet \\ \bullet & \bullet & \bullet & \bullet & \bullet & \bullet \end{array} \quad \mathcal{O}_3 = \begin{array}{cccccc} \bullet & \bullet & \bullet & \bullet & \bullet & \bullet \\ \bullet & \bullet & \bullet & \bullet & \bullet & \bullet \\ \bullet & \bullet & \bullet & \bullet & \bullet & \bullet \\ \bullet & \bullet & \bullet & \bullet & \bullet & \bullet \\ \bullet & \bullet & \bullet & \bullet & \bullet & \bullet \\ \bullet & \bullet & \bullet & \bullet & \bullet & \bullet \end{array}, \quad (31)$$

which shows  $(\mathcal{O}_2|\mathcal{O}_1) = 0$  and  $(\mathcal{O}_3|\mathcal{O}_2) = (\mathcal{O}_3|\mathcal{O}_0) = 0$ . In general, it follows that  $(\mathcal{O}_t|\mathcal{O}_{t+1}) = 0$ . If we define a matrix  $\mathcal{A}$  such that  $\mathcal{A}_{mm} = (\mathcal{O}_n|\mathcal{O}_m)$ , it is such that its odd off-diagonal terms are zero. We now prove that even off-diagonal terms are equal to each other. To show this consider

$$\begin{aligned} \mathcal{A}_{t,t-2} &\equiv (\mathcal{O}_t|\mathcal{O}_{t-2}) \propto \text{Tr}(\mathcal{O}_t^\dagger \mathcal{O}_{t-2}) \\ &= \text{Tr}(U^\dagger \mathcal{O}_{t-1}^\dagger U \mathcal{O}_{t-2}) \\ &= \text{Tr}(\mathcal{O}_{t-1}^\dagger \mathcal{O}_{t-3}) \equiv \mathcal{A}_{t-1,t-3}, \end{aligned}$$

as required. In summary, we can write

$$\mathcal{A} = \begin{bmatrix} 1 & 0 & \mathcal{A}_{0,2} & 0 & \mathcal{A}_{0,4} & \cdots \\ 0 & 1 & 0 & \mathcal{A}_{0,2} & 0 & \cdots \\ \mathcal{A}_{0,2} & 0 & 1 & 0 & \mathcal{A}_{0,2} & \cdots \\ 0 & \mathcal{A}_{0,2} & 0 & 1 & 0 & \cdots \\ \vdots & \cdots & \cdots & \cdots & \cdots & \vdots \end{bmatrix}. \quad (32)$$

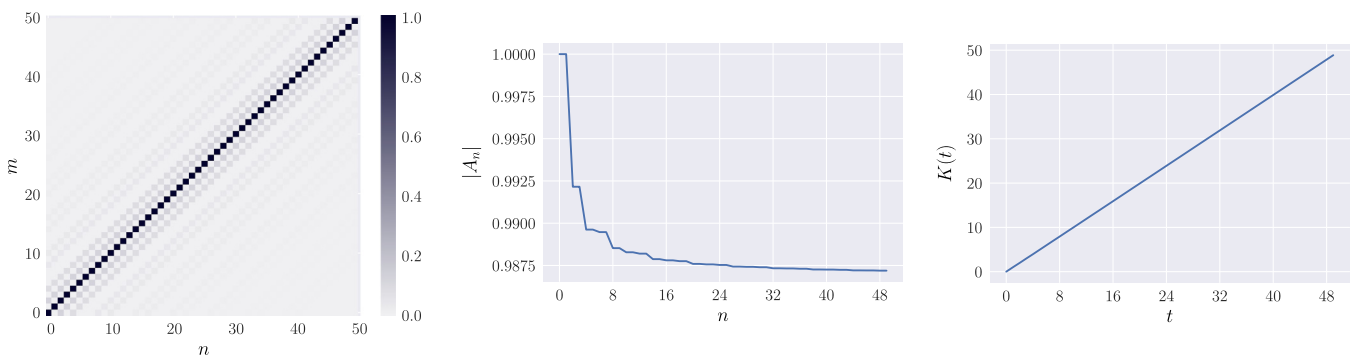


FIG. 5. The numerical analysis for the Krylov complexity of discrete-time quantum walk with coin-angle  $\theta = \pi/6$  and initial operator  $\sigma^x \otimes |0\rangle\langle 0|$ . (Left) The inner product matrix  $\mathcal{A}_{nm} = (\mathcal{O}_n|\mathcal{O}_m)$  whose elements odd off-diagonal elements are 0 while the even off-diagonal elements are equal. (Center) The norm of operator  $\{|A_n\rangle$  decays and then saturates to a value  $\mathcal{O}(1)$ . (Right) The K-complexity shows a linear growth.

Therefore, the Krylov basis vector  $|O_n\rangle$  is given by

$$|A_n\rangle = |\mathcal{O}_n\rangle - \sum_{i<n} (\mathcal{O}_i|\mathcal{O}_n)|\mathcal{O}_i\rangle \rightarrow |\mathcal{O}_n\rangle = \frac{|A_n\rangle}{\|A_n\|},$$

$$|A_0\rangle = |\mathcal{O}_0\rangle,$$

$$|A_1\rangle = |\mathcal{O}_1\rangle,$$

$$|A_2\rangle = |\mathcal{O}_2\rangle - \mathcal{A}_{02}|\mathcal{O}_0\rangle \rightarrow \|A_2\| = 1 - |\mathcal{A}_{02}|^2,$$

$$|A_3\rangle = |\mathcal{O}_3\rangle - \mathcal{A}_{02}|\mathcal{O}_1\rangle \rightarrow \|A_3\| = 1 - |\mathcal{A}_{02}|^2.$$

As the dispersion in discrete-time quantum walk grows linearly [63], the operator support on a particular site decays over time. Hence, the overlap between the initial operator  $\mathcal{O}_0$  and operator at any subsequent time  $\mathcal{O}_{2t}$  also decays over time. In other words,  $\mathcal{A}_{0,2t} \approx 0$ , and therefore,  $(\mathcal{O}_n|\mathcal{O}_m) \approx \delta_{nm}$ . It follows that  $\phi_{n,t} = (\mathcal{O}_n|\mathcal{O}_t) \approx \delta_{n,t}$ , hence the K-complexity given by

$$K(t) = \sum_n n |\phi_n(t)|^2 \sim t, \quad (33)$$

therefore, grows linearly. In Fig. 5, the numerical analysis is presented for the K-complexity of the discrete-time quantum walk. The norm of operator  $|A_n\rangle$  saturates at a constant value close to 1 showing that at late time, the operators  $|\mathcal{O}_n\rangle$  are approximately orthogonal to each other. Therefore, the K-complexity obeys a linear growth.

As we see in Sec. IV A, the introduction of disorder leads to the slowdown in information propagation. The K-complexity shows the similar localized behavior as the OTOC in which it deviates from linear growth to suppress the power law  $\sim t^{1/\delta}$  with  $\delta > 1$ . In this case, the amplitude  $\mathcal{A}_{0,2n}$  goes to zero for large  $n$  due to localization at  $n = 0$ . Therefore, the expansion coefficient  $\phi_{n,t} = (\mathcal{O}_n|\mathcal{O}_t)$  is nonzero for small  $n$  which results in suppressed growth in complexity. In Fig. 6, the K-complexity is calculated under temporal and spatial disorder in the discrete-time quantum walk for increasing disorder strength  $W$ . As with the OTOC, the suppression in the K-complexity growth is smaller in the temporal case compared to the spatial as a result of strong localization (or AL) in the latter case.

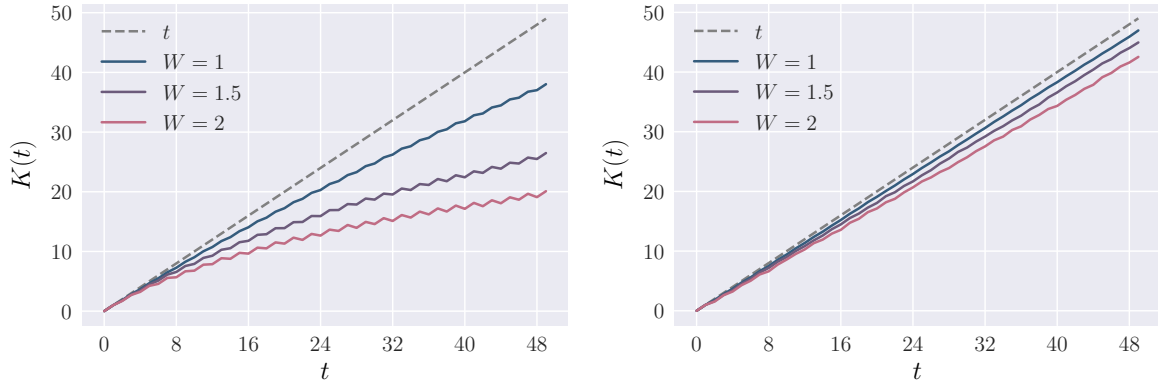


FIG. 6. The K-complexity calculated for discrete-time quantum walk in the presence of (Left) spatial. (Right) temporal disorder with varying disorder strength  $W$ . The disorder is taken over 500 copies. The dotted lines show the curve corresponding to  $y(t) = t$ .

## V. CONCLUSION

In summary, the discrete-time quantum walks are a quantum model which can be used to simulate a large number of phenomena from quantum many-body physics as well as for the construction of quantum algorithms. Their experimental implementation on a wide number of platforms makes them suitable to study theoretical ideas. In this article, we study information scrambling in the discrete-time quantum walk by using the out-of-time correlators and K-complexity as probes. The OTOC features the “shell-like” behavior, in which, at long-time limit, it goes to zero indicating no scrambling of the operator. The introduction of disorder (spatial or temporal) results in a slowdown of information scrambling where the shape of the light cone confines up to localization length. The K-complexity shows a linear growth which ties to the fact that the operator at any time is approximately orthonormal to all operators at previous times. The disorder suppresses the K-complexity growth resulting in its sublinear behavior. While the spatial disorder results in strong localization, the temporal disorder results in weak localization, which is apparent from the behavior of both OTOC as well as K-complexity.

We would like to understand the effect of boundary conditions. In this work, we focus on the discrete-time quantum walk in an infinite-dimensional one-dimensional (1D) lattice, but from the experimental point of view, it may be interesting to see the late-time behavior of these quantities  $t > L$ . In Ref. [75], the information scrambling was studied on Clifford quantum cellular automata (QCA). These systems were shown to break ergodicity, i.e., they exhibited quantum scarring. It was further shown that such a system could exhibit classical dynamics in some semi-classical limit. While the discrete-time quantum walks are not the same as QCA, they can be regarded as the dynamics of the one-particle sector of a QCA [76]. Therefore, it will be interesting to see if the connection between the two results can be made more direct. In this direction, one should note that the Clifford QCAs model studied in Ref. [75] also exhibits linear growth in K-

complexity. It follows from the evolution of the operator under Clifford QCAs in which a string of Pauli operators maps to another. Since the Pauli operator forms an orthonormal basis, each evolution step generates a new basis element resulting in linear growth. While for the infinite-dimensional case, this growth will persist forever due to the infinite-dimensional Hilbert space, in the case of the finite-dimensional lattice, the growth will stop as the operator gets back to its initial state. Therefore, the linear growth in K-complexity follows by a sudden decay to zero followed by repetitive behavior which is the refactoring of recurrence dynamics.

In this work, we formulate the K-complexity for the system with discrete-time evolution. Therefore, it opens up a way to consider more interesting many-body systems with discrete-time evolution. One such example could be random unitary circuits (RUCs) [77], which has been an active area of research for the past several years. RUCs have shed light on longstanding questions about thermalization and chaos and on the underlying universal dynamics of quantum information and entanglement [78]. While several works explored the dynamics of OTOC in a number of variants of RUCs [79,80], the study of K-complexity can further help understand postscrambling-time behavior.

From the point of view of discrete-time quantum walks, which are the basis of many quantum algorithms, the study of information scrambling could provide the basis for designing algorithms that can efficiently explore the Hilbert spaces. In this context, the K-complexity which describe the delocalization of the operator in Hilbert space may be useful. Overall, the study of scrambling in both discrete-time quantum walks as well as in more generic systems with discrete-time evolution paves the way toward new physics in quantum many-body physics.

## ACKNOWLEDGMENT

We wish to thank Aranya Bhattacharya for various useful discussions and comments about this and related works.

- [1] S. Xu and B. Swingle, *PRX Quantum* **5**, 010201 (2024).  
 [2] R. J. Lewis-Swan, A. Safavi-Naini, A. M. Kaufman, and A. M. Rey, *Nat. Rev. Phys.* **1**, 627 (2019).

- [3] J. M. Deutsch, *Phys. Rev. A* **43**, 2046 (1991).  
 [4] M. Rigol, V. Dunjko, and M. Olshanii, *Nature (London)* **452**, 854 (2008).



- [5] M. Srednicki, *Phys. Rev. E* **50**, 888 (1994).
- [6] J. Maldacena, S. H. Shenker, and D. Stanford, *J. High Energy Phys.* **08** (2016) 106.
- [7] Y. Sekino and L. Susskind, *J. High Energy Phys.* **10** (2008) 065.
- [8] N. Lashkari, D. Stanford, M. Hastings, T. Osborne, and P. Hayden, *J. High Energy Phys.* **04** (2013) 022.
- [9] S. H. Shenker and D. Stanford, *J. High Energy Phys.* **03** (2014) 067.
- [10] S. Sahu, S. Xu, and B. Swingle, *Phys. Rev. Lett.* **123**, 165902 (2019).
- [11] B. Swingle and D. Chowdhury, *Phys. Rev. B* **95**, 060201(R) (2017).
- [12] J. R. McClean, S. Boixo, V. N. Smelyanskiy, R. Babbush, and H. Neven, *Nat. Commun.* **9**, 4812 (2018).
- [13] J. Haferkamp, F. Montealegre-Mora, M. Heinrich, J. Eisert, D. Gross, and I. Roth, *Commun. Math. Phys.* **397**, 995 (2023).
- [14] H. Shen, P. Zhang, Y.-Z. You, and H. Zhai, *Phys. Rev. Lett.* **124**, 200504 (2020).
- [15] Y. Wu, P. Zhang, and H. Zhai, *Phys. Rev. Res.* **3**, L032057 (2021).
- [16] R. J. Garcia, K. Bu, and A. Jaffe, *J. High Energy Phys.* **03** (2022) 027.
- [17] B. Swingle, *Nat. Phys.* **14**, 988 (2018).
- [18] E. B. Rozenbaum, S. Ganeshan, and V. Galitski, *Phys. Rev. Lett.* **118**, 086801 (2017).
- [19] D. E. Parker, X. Cao, A. Avdoshkin, T. Scaffidi, and E. Altman, *Phys. Rev. X* **9**, 041017 (2019).
- [20] J. L. F. Barbón, E. Rabinovici, R. Shir, and R. Sinha, *J. High Energy Phys.* **10** (2019) 264.
- [21] E. Rabinovici, A. Sánchez-Garrido, R. Shir, and J. Sonner, *J. High Energy Phys.* **06** (2021) 062.
- [22] E. Rabinovici, A. Sánchez-Garrido, R. Shir, and J. Sonner, *J. High Energy Phys.* **07** (2022) 151.
- [23] E. Rabinovici, A. Sánchez-Garrido, R. Shir, and J. Sonner, *J. High Energy Phys.* **03** (2022) 211.
- [24] A. Bhattacharya, P. P. Nath, and H. Sahu, *Phys. Rev. D* **109**, 066010 (2024).
- [25] S.-K. Jian, B. Swingle, and Z.-Y. Xian, *J. High Energy Phys.* **03** (2021) 014.
- [26] B. Bhattacharjee, P. Nandy, and T. Pathak, *J. High Energy Phys.* **08** (2023) 099.
- [27] S. He, P. H. C. Lau, Z.-Y. Xian, and L. Zhao, *J. High Energy Phys.* **12** (2022) 070.
- [28] P. Caputa and S. Datta, *J. High Energy Phys.* **12** (2021) 188 [Erratum: **09** (2022) 113].
- [29] S. Khetrapal, *J. High Energy Phys.* **03** (2023) 176.
- [30] A. Kundu, V. Malvimat, and R. Sinha, *J. High Energy Phys.* **09** (2023) 011.
- [31] H. A. Camargo, V. Jahnke, K.-Y. Kim, and M. Nishida, *J. High Energy Phys.* **05** (2023) 226.
- [32] A. Avdoshkin, A. Dymarsky, and M. Smolkin, *J. High Energy Phys.* **03** (2024) 066.
- [33] J. Erdmenger, S.-K. Jian, and Z.-Y. Xian, *J. High Energy Phys.* **08** (2023) 176.
- [34] F. B. Trigueros and C.-J. Lin, *SciPost Phys.* **13**, 037 (2022).
- [35] P. H. S. Bento, A. del Campo, and L. C. Céleri, *Phys. Rev. B* **109**, 224304 (2024).
- [36] A. Bhattacharya, P. Nandy, P. P. Nath, and H. Sahu, *J. High Energy Phys.* **12** (2022) 081.
- [37] B. Bhattacharjee, X. Cao, P. Nandy, and T. Pathak, *J. High Energy Phys.* **03** (2023) 054.
- [38] A. Bhattacharya, P. Nandy, P. P. Nath, and H. Sahu, *J. High Energy Phys.* **12** (2023) 066.
- [39] C. Liu, H. Tang, and H. Zhai, *Phys. Rev. Res.* **5**, 033085 (2023).
- [40] B. Bhattacharjee, P. Nandy, and T. Pathak, *J. High Energy Phys.* **01** (2024) 094.
- [41] S. E. Venegas-Andraca, *Quantum Inf. Proc.* **11**, 1015 (2012).
- [42] A. Ambainis, *Int. J. Quantum Inf.* **01**, 507 (2003).
- [43] T. Oka, N. Konno, R. Arita, and H. Aoki, *Phys. Rev. Lett.* **94**, 100602 (2005).
- [44] S. Barkhofen, L. Lorz, T. Nitsche, C. Silberhorn, and H. Schomerus, *Phys. Rev. Lett.* **121**, 260501 (2018).
- [45] D. Xie, T.-S. Deng, T. Xiao, W. Gou, T. Chen, W. Yi, and B. Yan, *Phys. Rev. Lett.* **124**, 050502 (2020).
- [46] K. Manouchehri and J. Wang, *Physical Implementation of Quantum Walks* (Springer, Berlin, 2014).
- [47] M. Karski, L. Förster, J.-M. Choi, A. Steffen, W. Alt, D. Meschede, and A. Widera, *Science* **325**, 174 (2009).
- [48] M. A. Broome, A. Fedrizzi, S. Rahimi-Keshari, J. Dove, S. Aaronson, T. C. Ralph, and A. G. White, *Science* **339**, 794 (2013).
- [49] J. Wu, W.-W. Zhang, and B. C. Sanders, *Front. Phys.* **14**, 61301 (2019).
- [50] B. Swingle, G. Bentsen, M. Schleier-Smith, and P. Hayden, *Phys. Rev. A* **94**, 040302(R) (2016).
- [51] X. Mi, P. Roushan, C. Quintana, S. Mandrà, J. Marshall, C. Neill, F. Arute, K. Arya, J. Atalaya, R. Babbush, J. C. Bardin, R. Barends, J. Basso, A. Bengtsson, S. Boixo, A. Bourassa, M. Broughton, B. B. Buckley, D. A. Buell, B. Burkett *et al.*, *Science* **374**, 1479 (2021).
- [52] S. K. Zhao, Z.-Y. Ge, Z. Xiang, G.M. Xue, H.S. Yan, Z.T. Wang, Z. Wang, H.K. Xu, F.F. Su, Z.H. Yang, H. Zhang, Y.-R. Zhang, X.-Y. Guo, K. Xu, Y. Tian, H.F. Yu, D.N. Zheng, H. Fan, and S.P. Zhao, *Phys. Rev. Lett.* **129**, 160602 (2022).
- [53] M. Gärttner, J. G. Bohnet, A. Safavi-Naini, M. L. Wall, J. J. Bollinger, and A. M. Rey, *Nat. Phys.* **13**, 781 (2017).
- [54] J. Braumüller, A. H. Karamlou, Y. Yanay, B. Kannan, D. Kim, M. Kjaergaard, A. Melville, B. M. Niedzielski, Y. Sung, A. Vepsäläinen, R. Winik, J. L. Yoder, T. P. Orlando, S. Gustavsson, C. Tahan, and W. D. Oliver, *Nat. Phys.* **18**, 172 (2022).
- [55] K. A. Landsman, C. Figgatt, T. Schuster, N. M. Linke, B. Yoshida, N. Y. Yao, and C. Monroe, *Nature (London)* **567**, 61 (2019).
- [56] S. Xu and B. Swingle, *Nat. Phys.* **16**, 199 (2020).
- [57] S. Xu and B. Swingle, *Phys. Rev. X* **9**, 031048 (2019).
- [58] V. Khemani, D. A. Huse, and A. Nahum, *Phys. Rev. B* **98**, 144304 (2018).
- [59] V. Balasubramanian, P. Caputa, J. M. Magan, and Q. Wu, *Phys. Rev. D* **106**, 046007 (2022).
- [60] P. Suchsland, R. Moessner, and P. W. Claeys, *arXiv:2308.03851*.
- [61] D. W. Berry, A. M. Childs, R. Cleve, R. Kothari, and R. D. Somma, *Phys. Rev. Lett.* **114**, 090502 (2015).
- [62] C. M. Chandrashekar, *Sci. Rep.* **3**, 2829 (2013).
- [63] C. M. Chandrashekar, *arXiv:1212.5984*.
- [64] C. M. Chandrashekar, R. Srikanth, and R. Lafamme, *Phys. Rev. A* **77**, 032326 (2008).
- [65] C. M. Chandrashekar, *Phys. Rev. A* **83**, 022320 (2011).

- [66] L. A. Toikka, *Phys. Rev. B* **101**, 064202 (2020).
- [67] I. Vakulchyk, M. V. Fistul, P. Qin, and S. Flach, *Phys. Rev. B* **96**, 144204 (2017).
- [68] M. Malishava, I. Vakulchyk, M. Fistul, and S. Flach, *Phys. Rev. B* **101**, 144201 (2020).
- [69] M. Zeng and E. H. Yong, *Sci. Rep.* **7**, 12024 (2017).
- [70] N. P. Kumar, S. Banerjee, and C. M. Chandrashekar, *Sci. Rep.* **8**, 8801 (2018).
- [71] R. Vieira, E. P. M. Amorim, and G. Rigolin, *Phys. Rev. Lett.* **111**, 180503 (2013).
- [72] C.-J. Lin and O. I. Motrunich, *Phys. Rev. B* **97**, 144304 (2018).
- [73] A. Nayak and A. Vishwanath, [arXiv:quant-ph/0010117](https://arxiv.org/abs/quant-ph/0010117).
- [74] F. Evers and A. D. Mirlin, *Rev. Mod. Phys.* **80**, 1355 (2008).
- [75] B. Kent, S. Racz, and S. Shashi, *Phys. Rev. B* **107**, 144306 (2023).
- [76] T. Farrelly, *Quantum* **4**, 368 (2020).
- [77] M. P. Fisher, V. Khemani, A. Nahum, and S. Vijay, *Annu. Rev. Condens. Matter Phys.* **14**, 335 (2023).
- [78] A. Nahum, J. Ruhman, S. Vijay, and J. Haah, *Phys. Rev. X* **7**, 031016 (2017).
- [79] A. Nahum, S. Vijay, and J. Haah, *Phys. Rev. X* **8**, 021014 (2018).
- [80] Z. Weinstein, S. P. Kelly, J. Marino, and E. Altman, *Phys. Rev. Lett.* **131**, 220404 (2023).